Interferon γ–Induced Human Guanylate Binding Protein 1 Inhibits Mammary Tumor Growth in Mice

Karoline Lipnik,[1,2] Elisabeth Naschberger,[3] Nathalie Gonin-Laurent,[3] Petra Kodajova,[1] Helga Petznek,[1] Stefanie Rungaldier,[1] Simonetta Astigiano,[4] Silvano Ferrini,[4] Michael Stürzl,[3] and Christine Hohenadl[1]*

[1]Institute of Virology, Department of Pathobiology, University of Veterinary Medicine Vienna, Vienna, Austria; [2]Centre of Biomolecular Medicine and Pharmacology, Department of Vascular Biology and Thrombosis Research, Medical University Vienna, Vienna, Austria; [3]Division of Molecular and Experimental Surgery, Department of Surgery, University of Erlangen-Nuremberg, Erlangen, Germany; [4]Transgenic Unit and Immunotherapy Unit, Instituto Nazionale per la Ricerca sul Cancro, Genoa, Italy

Interferon γ (IFN-γ) has recently been implicated in cancer immunosurveillance. Among the most abundant proteins induced by IFN-γ are guanylate binding proteins (GBPs), which belong to the superfamily of large GTPases and are widely expressed in various species. Here, we investigated whether the well-known human GBP-1 (hGBP-1), which has been shown to exert antiangiogenic activities and was described as a prognostic marker in colorectal carcinomas, may contribute to an IFN-γ–mediated tumor defense. To this end, an IFN-independent, inducible hGBP-1 expression system was established in murine mammary carcinoma (TS/A) cells, which were then transplanted into syngeneic immune-competent Balb/c mice. Animals carrying TS/A cells that had been given doxycycline for induction of hGBP-1 expression revealed a significantly reduced tumor growth compared with mock-treated mice. Immunohistochemical analysis of the respective tumors demonstrated a tightly regulated, high-level expression of hGBP-1. No signs of an enhanced immunosurveillance were observed by investigating the number of infiltrating B and T cells. However, hemoglobin levels as well as the number of proliferating tumor cells were shown to be significantly reduced in hGBP-1–expressing tumors. This finding corresponded to reduced amounts of vascular endothelial growth factor A (VEGF-A) released by hGBP-1–expressing TS/A cells *in vitro* and reduced VEGF-A protein levels in the corresponding mammary tumors *in vivo*. The results suggest that hGBP-1 may contribute to IFN-γ–mediated antitumorigenic activities by inhibiting paracrine effects of tumor cells on angiogenesis. Consequently, owing to these activities GBPs might be considered as potent members in an innate, IFN-γ–induced antitumoral defense system.

Online address: http://www.molmed.org
doi: 10.2119/molmed.2009.00172

INTRODUCTION

The type II interferon, interferon γ (IFN-γ), has recently been implicated in cancer immunosurveillance in addition to its well-known function in promoting host responses to microorganisms (reviewed in [1]). According to a number of different experiments in mice, IFN-γ participates in immunoediting, which describes the interaction of the host's immune system with emerging tumors (2). Experimental data generated with IFN-γ–insensitive mice, deficient for either an IFN-γ receptor subunit or the respective signal transduction pathway (3,4), indicated that in wild-type mice endogenously produced IFN-γ not only promotes rejection of transplantable tumors, but also prevents development of primary tumors. Although natural killer (NK) cells, NK T cells and apoptosis-mediating ligands such as TRAIL (tumor necrosis factor–related apoptosis-inducing ligand) have been shown to be involved in this process (2), the detailed cellular and molecular levels of the cancer-eliminating phase still remain to be elucidated. In this respect, Kundu and colleagues (5,6) previously reported interleukin (IL)-10–induced antitumoral activity in a mammary cancer mouse model. Follow-up studies revealed a substantial role of IFN-γ in this process (7). Interestingly, during these experiments, the upregulation of two IFN-γ–inducible genes, *mig-1* and *gbp-1*, within the transplanted tumor cells was demonstrated. Mig-1, the monokine induced by IFN-γ or CXCL9, is known to attract activated T and NK cells and was recently shown to at least partially contribute to the observed limited metastasis within the investigated tumor model (8). The role of the IFN-γ–induced guanylate binding protein (GBP), however, remained unclear.

Address correspondence and reprint requests to *Christine Hohenadl, Institute of Virology, Department of Pathobiology, University of Veterinary Medicine Vienna, Veterinaerplatz 1, A-1210 Vienna, Austria. Phone: +431250772330; Fax: +431250772390; E-mail: christine.hohenadl@vetmeduni.ac.at.*
Submitted November 20, 2009; accepted for publication February 4, 2010; Epub (www.molmed.org) ahead of print February 5, 2010.

GBPs were originally identified in human fibroblasts as the most abundant proteins induced by IFN-γ treatment (9). The GBPs are part of a subfamily within the protein superfamily of large GTPases including dynamins and Mx proteins (for a review see [10]). To date, 7 and 11 highly homologous GBPs with a relative molecular mass of 65–71 kDa have been identified in humans and mice, respectively (11–13). Human GBP-1 (hGBP-1), with respect to structure and function, is the best-characterized member within this family of proteins (14,15). Despite a detailed knowledge of biochemical characteristics, however, the biological functions of GBPs remain obscure. Recent studies focusing on hGBP-1 suggested that the protein mediates the inhibitory effects of inflammatory cytokines on proliferation, migration and invasiveness of endothelial cells (16–19). The antiangiogenic activity of hGBP-1 has been recently demonstrated for colorectal carcinomas. In a study investigating more than 380 tumor samples, it was shown that tumors expressing hGBP-1 exhibited reduced angiogenic activity, and this was associated with a significantly improved prognosis for the respective patients (20). In addition, an effect on proliferation of fibroblasts has been demonstrated for murine GBP-2 (21). These observations indicate that GBPs can alter cell growth and are able to modulate cellular interactions with their environment.

Thus, in the present study, the effects of hGBP-1 on tumor growth were investigated using an immune-competent mouse model of mammary cancer. To this aim, a tetracycline-regulated, IFN-independent hGBP-1 expression system was established in the highly malignant mouse mammary cancer cell line TS/A, followed by generation of respective tumors in syngeneic Balb/c mice. The impact of hGBP-1 on tumor cell proliferation, immune cell extravasation and angiogenesis was analyzed, revealing a highly significant tumor growth–inhibiting effect of hGBP-1, which appeared to be due to a defect in angiogenesis rather than to enhanced tumor immunosurveillance.

MATERIALS AND METHODS

Cells and Plasmids

The murine adenocarcinoma cell line TS/A, which was derived from a spontaneous mammary cancer of Balb/c mice (22), was cultured in RPMI 1640 (Invitrogen Life Technologies, Carlsbad, CA, USA) supplemented with 1% nonessential amino acids, 2 mmol/L glutamine and 10% fetal bovine serum (FBS) (all Invitrogen Life Technologies). Cells were maintained at 37°C with 5% CO_2 and 95% humidity. To establish an inducible expression system, cells were transduced with the murine leukemia virus (MLV)-derived retroviral vector pLib-rtTA-M2-IRES-TRSID-IRES-Puro^r containing a tetracycline on/off regulatory system (23,24). The coding sequence of hGBP-1 was isolated from pMCV1.4 + GBP-1 (25) by restriction digestion with *Eco*RI and inserted into the linearized tetracycline response plasmid pUHD10.3 (24). In addition, a SV40 promoter–driven hygromycin selection cassette (24) was inserted via the restriction sites *Pci*I and *Nar*I, finally giving rise to the inducible expression vector pUHD10.3-GBP-Hyg (pUHD-GBP). As a control, the plasmid pUHD10.3-Hyg lacking the hGBP-1 encoding sequence (pUHD) was also generated. Stably transfected cell clones and populations were selected by addition of hygromycin (200 μg/mL) and puromycin (10 μg/mL), respectively. Expression of hGBP-1 was induced by addition of 1–2.5 μg/mL doxycycline (Sigma-Aldrich, St. Louis, MO, USA), a tetracycline homolog.

Proliferation Assay

A population of TS/A cells as well as isolated single cell clones, stably transfected with pUHD-GBP, and a population of cells transfected with the control vector pUHD were seeded in six-well plates (duplicates) at a density of 1×10^5 cells/well. The next day, 1 μg/mL (low-level hGBP-1 expression) or 2.5 μg/mL (high-level hGBP-1 expression) doxycycline was added to the cell culture medium. For cells that were treated with doxycycline for more than 24 h, fresh doxycycline was added daily. Cells were incubated for 24, 48, 72 and 96 h. At these time points, cells were harvested, and total cell numbers (cells/well) were determined by use of a CasyTT® cell counter (Schärfe System, Reutlingen, Germany). For determination of potential effects of hGBP-1 expression on proliferation, cell numbers were compared with cells that did not receive doxycycline (nontreated control). Mean values ± SD were calculated from three independent experiments.

Soft Agar Assay

To investigate tumorigenicity of TS/A cells (nontransfected and transfected with the control vector pUHD) in comparison to pUHD-GBP–transfected cell clones (clones 14 and 18, mixed 1:1) *in vitro*, growth in soft agar was evaluated. To this end, the wells of a six-well plate were coated with a solution of RPMI 1640/10% FBS containing 0.5% agar (Difco, Detroit, MI, USA) as well as either 1 or 2.5 μg/mL doxycycline. Once this layer was set, 2×10^4 cells/well (triplicates) embedded in RPMI 1640/10% FBS/0.3% agar containing either 1 or 2.5 μg/mL doxycycline were seeded on top. Cells were allowed to grow for 8 d, at which point they were stained with 0.005% crystal violet and the average number of colonies determined by analyzing 10 different optical fields (Zeiss Axiovert 200M, Carl Zeiss GmbH, Vienna, Austria; magnification 100×). Mean values and SD were calculated.

Western Blot Analysis

Proteins extracted from cells or tissues were quantified by applying a modified Lowry assay (Bio-Rad DC protein assay, Bio-Rad Laboratories, Vienna, Austria) using bovine serum albumin (Promega, Mannheim, Germany) as a reference standard. Equal amounts of protein were then separated under reducing conditions in 10% SDS-polyacrylamide gels

and transferred onto a Hybond-P polyvinyldifluoride (PVDF) membrane (GE Healthcare Technologies, Vienna, Austria). Membranes were blocked for 1 h in 5% organic skim milk powder (Heiler Cenovis, Radolfzell, Germany) dissolved in phosphate-buffered saline (PBS) (VWR International, West Chester, PA, USA) containing 0.1% Tween-20 (Bio-Rad). Detection of hGPP-1 was performed as described (26). Briefly, membranes were incubated for 1 h in PBS/0.1% Tween-20/5% milk powder containing a 1:500 diluted rat monoclonal anti–hGBP-1 antibody. Bound antibody was detected by applying a species-specific horseradish peroxidase (HRP)-conjugated secondary antibody (Dako Cytomation, Vienna, Austria) (diluted 1:10,000) followed by enhanced chemiluminescence (GE Healthcare). For staining of murine vascular endothelial growth factor (VEGF), a rabbit polyclonal antiserum recognizing the different variants of mouse and human VEGF-A (Santa Cruz Biotechnology, Heidelberg, Germany) was applied in a dilution of 1:400. As an internal control allowing evaluation of loaded protein amounts, glyceraldehyde-3-phosphate dehydrogenase (GAPDH) was detected using a monoclonal mouse anti-GAPDH antibody (Millipore-Chemicon International, Vienna, Austria) (diluted 1:50,000). For quantification of protein levels, linear exposures of blotted membranes were scanned using a fluoroimager (Storm 860; Amersham Biosciences [GE Healthcare Europe, Freiburg, Germany]), and bands were evaluated applying the respective analysis software (ImageQuant TL, GE Healthcare Europe).

Tumor Mouse Model

Cells (1×10^6) of stably transfected/infected TS/A cells harboring either the doxycycline-inducible expression vector pUHD10.3-GBP-Hyg (cell clones 14 and 18, mixed 1:1) or the parental vector pUHD10.3-Hyg (cell population), were injected subcutaneously into the pectoral mammary fat pad of female, 8-wk-old Balb/c mice (40 animals per cell type) (Jackson Laboratories, Bar Harbor, ME, USA). All animals were implanted subcutaneously with a microchip transponder (BackHome; Virbac, Vienna, Austria) for individual identification. At d 7 after injection, mice were randomly distributed into two groups. One group (treated) was injected intraperitoneally with doxycycline at a concentration of 50 mg/kg body weight (27) every 12 h for the first 72 h and every 24 h thereafter. The other group (nontreated) was injected in the same way with physiological saline solution (0.9% NaCl). Tumors were measured three times a wk in two dimensions, using a caliper, and the tumor volume was calculated according to the formula $L \times w \times w/2$. Evaluation of tumor growth was performed in a blinded manner, knowing only the identification number but not the group affiliation of the respective animals. The experiment was stopped 17 d after onset of induction, when tumor sizes exceeded 1500 mm^3. Mice were killed by cervical dislocation and dissected. Tumor tissue was frozen in liquid nitrogen and stored at –80°C until use or was fixed in 10% neutral buffered formalin (Sigma-Aldrich) for histological examination. Tumor growth in mice was performed according to the rules and regulations governing animal experimentation in Austria (BMBWK-68.205/0126-BrGT/2005).

Statistical Analysis

Tumor growth rates (doubling times) of individual animals in each experimental group were determined by nonlinear regression analysis of the obtained growth curves, shown as mean tumor volumes ± SEM. A two-tailed, unpaired Student *t* test (GraphPad Prism® software, GraphPad Software Inc., La Jolla, CA, USA) was used to determine the significance of differences between mean tumor doubling times of two experimental groups (doxycycline-treated versus nontreated control). The difference was considered statistically significant when $P < 0.05$.

Immunohistochemistry

Tumor samples fixed in 10% neutral buffered formalin (Sigma-Aldrich) or zinc fixative (BD Pharmingen, part of BD Biosciences, Heidelberg, Germany) were embedded in paraffin (Histo-Comp®; Sanova, Vienna, Austria) using automatic embedding equipment (Tissue Tek; Miles Scientific, Vienna, Austria). Subsequently, 5-μm sections were prepared, dewaxed in xylol (ACM Handels, Vienna, Austria) and rehydrated in a descending ethanol series (100%, 96% and 70%). After antigen retrieval by microwave pretreatment (3 × 7 min, 580 W) in target retrieval solution, pH 9 (TRS9; Dako), slides were treated with 7.5% hydrogen peroxide for 10 min at room temperature to block endogenous peroxidases. For staining of hGBP-1, slides were incubated for 1 h with monoclonal rat anti–hGBP-1 (1:300) at room temperature. Subsequently, sections were incubated for 30 min with biotinylated horse antirat IgG, followed by 30 min of incubation with an avidin-biotin complex (ABC kit; Vector Laboratories, Burlingame, CA). The reaction was developed with 0.1% 3,3′-diaminobenzidine (DAB) hydrochloride (Sigma-Aldrich) in 0.03% hydrogen peroxide and counterstained with Mayer's hemalum (VWR International). After dehydration for 2 min in ethanol (96% and 100%) and 2-min incubation in xylol, sections were mounted in DPX mounting medium (Sigma-Aldrich) and examined by light microscopy (Zeiss Axiovert 200M). Staining for the mouse endothelial cell–specific marker CD31 and the proliferation marker Ki-67 was performed on zinc-fixed tissue sections (28,29) using monoclonal rat antimouse CD31 (clone MEC 13.3; Santa Cruz) diluted 1:250) and rat antimouse Ki-67 antibodies (Tec-3; Dako Cytomation) (diluted 1.50). Staining was visualized using a species-specific APAAP (alkaline phosphatase anti–alkaline phosphatase) detection system applying fuchsin (Dako Cytomation) as a substrate. Sections were counterstained with hematoxylin Gill-III (Merck, Darmstadt, Germany) and mounted. Quantitative evaluation of proliferating cells

within tumor sections (GBP^+, $n = 11$; GBP^-, $n = 10$) was performed using the AxioVision version 1.4 software (Zeiss). Therefore, sections were photographed (Zeiss Axiovert 200M, magnification 100×) and aligned to consecutive sections stained for hGBP-1 expression. The respective tumor area was divided into individual squares to facilitate counting of Ki-67–positive cells/100,000 μm^2 in regions with high or low hGBP-1 expression. Subsequently, mean values and respective SDs were calculated. Results were statistically analyzed as described above, applying either an unpaired Student *t* test or, if more than two groups were compared, a one-way ANOVA.

For detection of B and T cells in tumor sections, slides were dewaxed and hydrated as described above. Antigen retrieval was performed by boiling samples in citrate buffer pH 6.0 (3 × 5 min in a microwave oven). As primary antibodies, a rabbit monoclonal anti-CD3 (clone SP7; Lab Vision-Neomarkers, Fremont, CA, USA), diluted 1:50, and a rat monoclonal anti-CD45R/B220 (BD Pharmingen), diluted 1:25, were used. Species-specific secondary antibodies were biotinylated (Dako Cytomation), and antigen reaction was revealed with HRP-conjugated streptavidin (Bio SPA, Milan, Italy) and DAB as a substrate (Lab Vision).

Positively stained cells in eight different sections were counted blindly by evaluating 10 different randomly chosen optical fields at a magnification of 400×. Results are given as mean values ± SD.

Determination of Hemoglobin Contents

To determine the level of perfusion in explanted tumors (30), snap-frozen tissue samples (TS/A-GBP + doxycycline, $n = 18$; TS/A-GBP – doxycycline and TS/A-Hyg + doxycycline, $n = 18$) were weighed and pulverized under liquid nitrogen using a pestle and mortar. Powdered tissue was suspended in water for injection (100 μL/10 mg tissue) and centrifuged at 16110*g* at 4°C for 5 min (Eppendorf centrifuge 5415R), and total protein contents were determined for normalization as described above. To quantify the hemoglobin content, 100 μL of the tumor suspension was mixed with 900 μL Drabkin's reagent (Sigma-Aldrich) and incubated in the dark at room temperature for 15 min. As a reference, human hemoglobin (30–160 mg/mL) (Sigma-Aldrich) was used. Absorbance was measured using a spectrophotometer at 540 nm. Statistical evaluation was performed by use of an unpaired Student *t* test as described above.

VEGF-ELISA

For analysis of synthesis of murine VEGF, tetracycline (Tet)-regulated TS/A cells stably transfected with pUHD10.3-hGBP-Hyg (cell clones 14 and 18) as well as cells transfected with the control vector pUHD10.3-Hyg were seeded in duplicates into six-well plates at a density of 1×10^5 cells/well. The next day, and daily thereafter, either 1 or 2.5 μg/mL doxycycline was added to the cell culture medium (RPMI/5% FBS). Non–doxycycline-treated cells were used as a control. All cells were cultured for 96 h, after which culture supernatants were harvested and filtered (Millipore, 0.45 μm), and the amount of secreted VEGF-A was determined using the Quantikine Mouse VEGF enzyme-linked immunosorbent assay (ELISA) (R&D Systems, Minneapolis, MN, USA), according to supplier's instructions. Samples were analyzed at 450 nm using an ELISA plate reader (Tecan GENios; Tecan, Männedorf, Austria). For normalization, cell numbers of each sample were determined (CasyTT®; Schärfe System, Reutlingen, Germany) and protein measurements (pg/mL) calculated according to 1×10^6 cells. Results are given as mean values ± SD.

RESULTS

Establishment and Characterization of TS/A Mouse Mammary Tumor Cells with Inducible hGBP-1 Expression

To generate an inducible hGBP-1–expressing tumor cell line, the mouse mammary adenocarcinoma cell line TS/A was first transduced with an MLV-derived retroviral vector encoding a tetracycline (Tet) on/off regulator system (23,24). The resulting cell population was subsequently transfected with the corresponding Tet-responsive expression vector pUHD10.3-GBP-Hyg (pUHD-GBP), giving rise to single cell clones which were then tested for inducible hGBP-1 expression upon treatment with doxycycline, a commonly used tetracycline derivative. Western blot analysis was performed to identify distinct cell clones, showing a tightly regulated high-level expression of hGBP-1 exclusively upon doxycycline treatment (Figure 1A).

To investigate potential effects of hGBP-1 expression *in vitro*, single cell clones as well as a population of TS/A cells stably transfected with pUHD-GBP were analyzed for their proliferation characteristics (Figure 1B). As a control, cells stably transfected with the expression vector lacking the hGBP-1 encoding sequence (pUHD) were analyzed. Cells were either left untreated (data not shown, 100% values) or incubated for 24 to 96 h with 1 or 2.5 μg/mL doxycycline. Finally, cell numbers were determined and calculated relative to untreated control cells (Figure 1B). The results show that hGBP-1 expression does not affect proliferation of the investigated cells *in vitro*. Similarly, no effects of hGBP-1 expression were observed on the potential of transfected TS/A cells to form colonies in soft agar (Figure 1C), indicating that hGBP-1 alters neither tumorigenicity nor metastatic potential of these cells.

hGBP-1 Expression Inhibits Growth of TS/A Cell–Derived Tumors in Balb/c Mice

After analysis of the growth characteristics of the established stably transfected TS/A cells *in vitro*, two tightly regulated cell clones that expressed high levels of hGBP-1 upon doxycycline treatment (see Figure 1A) were equally mixed and injected subcutaneously into the mammary fat pad of immune-

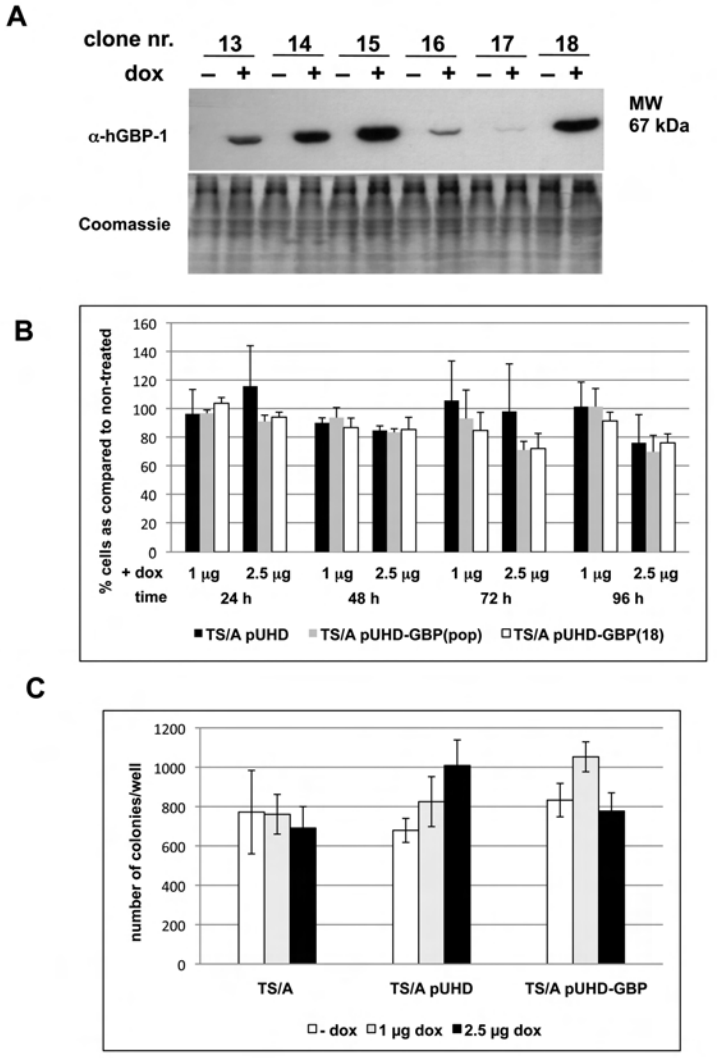

Figure 1. Characterization of TS/A mammary carcinoma cells inducibly expressing hGBP-1. (A) Western Blot analysis of TS/A cell clones 13–18 harboring the Tet on/off regulatory system and the vector pUHD10.3-GBP-Hyg, mediating tightly regulated, inducible expression of hGBP-1 in response to doxycycline (+ dox). As a control for analysis of equal amounts of protein, a Coomassie-stained SDS-polyacrylamide gel with the respective samples is depicted (lower panel). (B) Analysis of proliferation characteristics of pUHD10.3-GBP–transfected cells (cell population, gray bars; cell clone, white bars) in comparison to pUHD10.3-Hyg–transfected cells (black bars). Cell numbers (mean values ± SD) from three independent experiments are shown in % relative to nontreated (– dox) samples. (C) Soft agar assay. Nontransfected TS/A cells and TS/A cells transfected with pUHD10.3-Hyg or the hGBP-1–encoding vector (pUHD10.3-GBP) were analyzed for their ability to form colonies in soft agar. Expression of hGBP-1 was induced by addition of 1 (gray bars) or 2.5 (black bars) µg/mL doxycycline and the number of colonies (mean values ± SD) obtained by counting 10 different optical fields compared with nontreated samples (white bars).

competent syngeneic Balb/c mice to investigate the effects of hGBP-1 expression on TS/A cell–derived tumors *in vivo*. As a control, a population of cells stably transfected with the vector pUHD10.3-Hyg (pUHD) was also injected. After 7 d, when tumor volumes had reached 100 mm^3, mice were split into two groups ($n = 20$) and injected intraperitoneally with either doxycycline (+ dox) or saline (– dox). Tumor growth was regularly measured, and the experiment was stopped when tumor volumes exceeded 1500 mm^3. Mice that did not develop tumors at the end of the experiment ($n = 4$) or died of other causes ($n = 2$) were excluded from the analyses. Significantly reduced tumor growth ($P = 0.025$) was shown in mice that were injected with pUHD-GBP–transfected cells and had been given doxycycline compared with animals that were injected with saline (Figure 2A). An even more pronounced effect ($P = 0.009$) was observed when tumor growth of hGBP-1–expressing cells (TS/A pUHD-GBP + dox) was compared with that of cells transfected with the parental vector (see Figure 2A). Application of doxycycline did not have any effect on tumor growth as demonstrated by equal growth rates of pUHD-transfected cells in both doxycycline- and saline-treated mice (see Figure 2A).

At the end of the experiment, animals were killed, and tumors were excised for further analyses. Expression of hGBP-1 was shown by immunohistochemical analyses of excised tumor tissue using a monoclonal antibody specific for the human protein (26). All tumors derived from doxycycline-treated mice that had been injected with pUHD-GBP-transfected TS/A cells showed strong expression of hGBP-1 in tumor cells (Figure 2B, a and b). Tumors derived from pUHD-GBP–transfected TS/A cells that had been treated with saline, on the other hand, showed only single tumor cells positively stained for the presence of hGBP-1 protein (Figure 2B, c). No unspecific staining was observed in tumors derived from pUHD-transfected TS/A cells (Figure 2B, d).

Tumor Cell Proliferation Is Reduced in High-Level hGBP-1–Expressing Tumors

To elucidate the cause of hGBP-1 expression–associated reduced tumor growth, the excised tissue was analyzed for the presence of Ki-67, a common cellu-

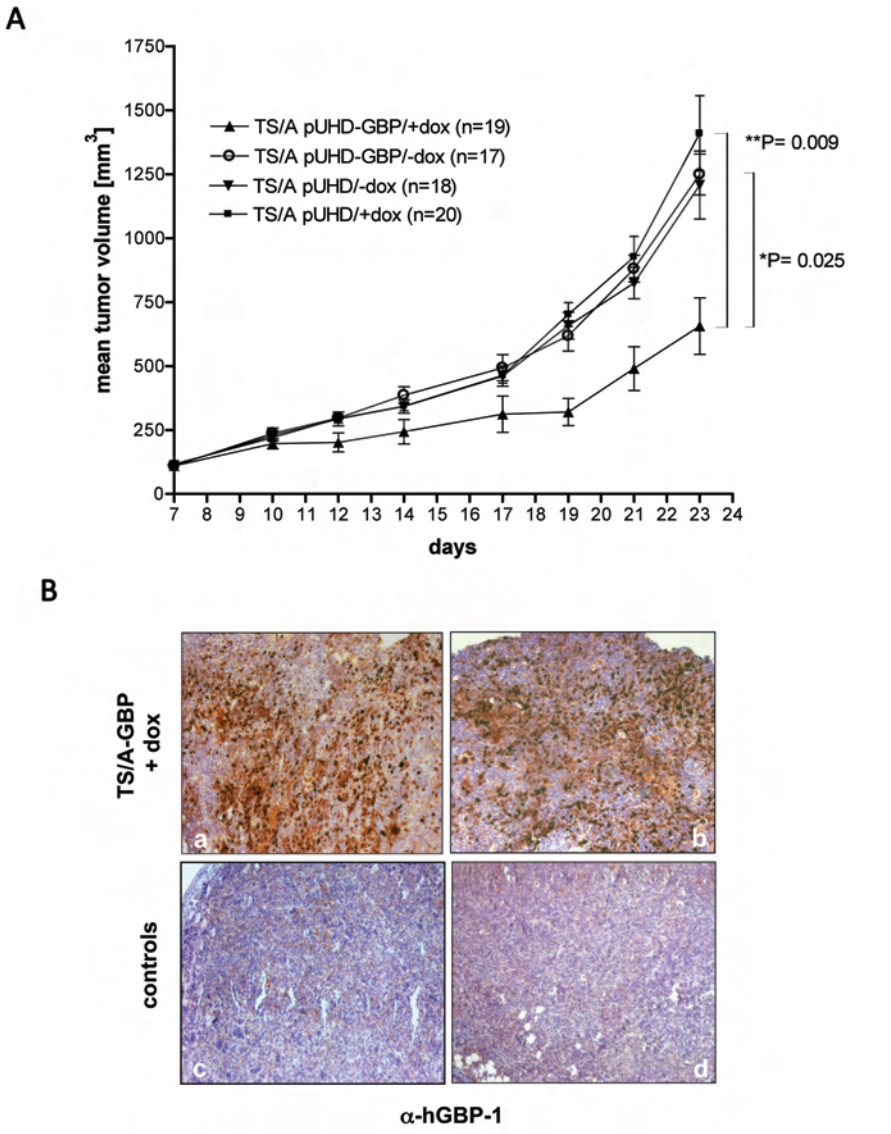

Figure 2. Effect of hGBP-1 expression on tumor growth in a syngeneic mammary carcinoma mouse model. (A) Tumor growth was monitored in Balb/c mice injected with 1 × 10^6 TS/A cells transfected with either pUHD10.3-GBP (▲, ○) or the parental vector pUHD10.3-Hyg (▼, ■). At d 7 after injection, animals were divided into two groups (n = 20) given either doxycycline (+ dox) or saline (– dox). Mean tumor volumes (± SEM) of individual animals are indicated. Animals that did not develop a tumor at the end of the experiment or died due to unrelated reasons were excluded. Statistical significance (P values) was determined applying a Student t test comparing the tumor doubling times of doxycycline-treated versus nontreated animals. (B) hGBP-1–specific immunohistochemical analysis of tumors derived from pUHD-GBP–transfected TS/A cells treated with doxycycline (a, b) or saline (c). No unspecific staining was observed in tumors from doxycycline-treated animals that had been injected with TS/A cells harboring the control vector pUHD (d).

lar marker indicating cell proliferation (31). To this end, hGBP-1–expressing (n = 11) and nonexpressing (n = 10) tumors were immunohistochemically stained with a specific antibody detecting murine Ki-67 (Figure 3A). The number of Ki-67–positive cells was evaluated by analyzing at least four different areas of a given section using the Zeiss AxioVision software (Figure 3A, area report). By this means, a significantly (P = 0.0175) reduced number of proliferating tumor cells/100,000 μm^2 was shown in hGBP-1–expressing tumors (Figure 3B). Analysis of consecutive sections for hGBP-1 expression and Ki-67 (see Figure 3A) allowed an assignment of cell proliferation with hGBP-1 expression. This approach showed that inhibition of cell proliferation is predominantly observed in areas with high GBP-1 expression (see Figure 3B). In contrast, reduced cell proliferation was hardly observed in tissues with a low level of hGBP-1 expression and was not observed in tumors lacking hGBP-1 expression (see Figure 3B). Statistical evaluation comparing numbers of Ki-67–positive cells in high-level hGBP-1–expressing areas to all other investigated samples revealed a highly significant decrease (P < 0.0001) (see Figure 3B).

Inhibition of tumor cell proliferation as a result of hGBP-1 expression, however, was not encountered in the respective *in vitro* studies (see Figure 1B). Thus, based on previous reports showing that hGBP-1 exerts antiangiogenic effects *in vitro* and *in vivo* (17–19) and is robustly induced by IFN-γ, which in turn is implicated in tumor immunosurveillance (1,32), a possible contribution of these processes was investigated.

hGBP-1–Mediated Tumor Growth Inhibition Is Not due to a Specific Immune Reaction

Because an IFN-γ–stimulated immune response has been previously implicated in inhibition of mammary cancer cell–derived tumor growth in Balb/c mice (7,8), the hGBP-1–expressing TS/A cell–derived tumors generated in the present study were analyzed for evidence of immune stimulation by staining tissue sections for the presence of the cell-surface marker molecules CD3 and B220, indicating infiltration of tumors with T and B cells, respectively. CD3$^+$ cells were detected in the periphery of analyzed sections, predominantly in the vicinity of larger vessels, whereas B220$^+$ B cells were barely detectable (Figure 4,

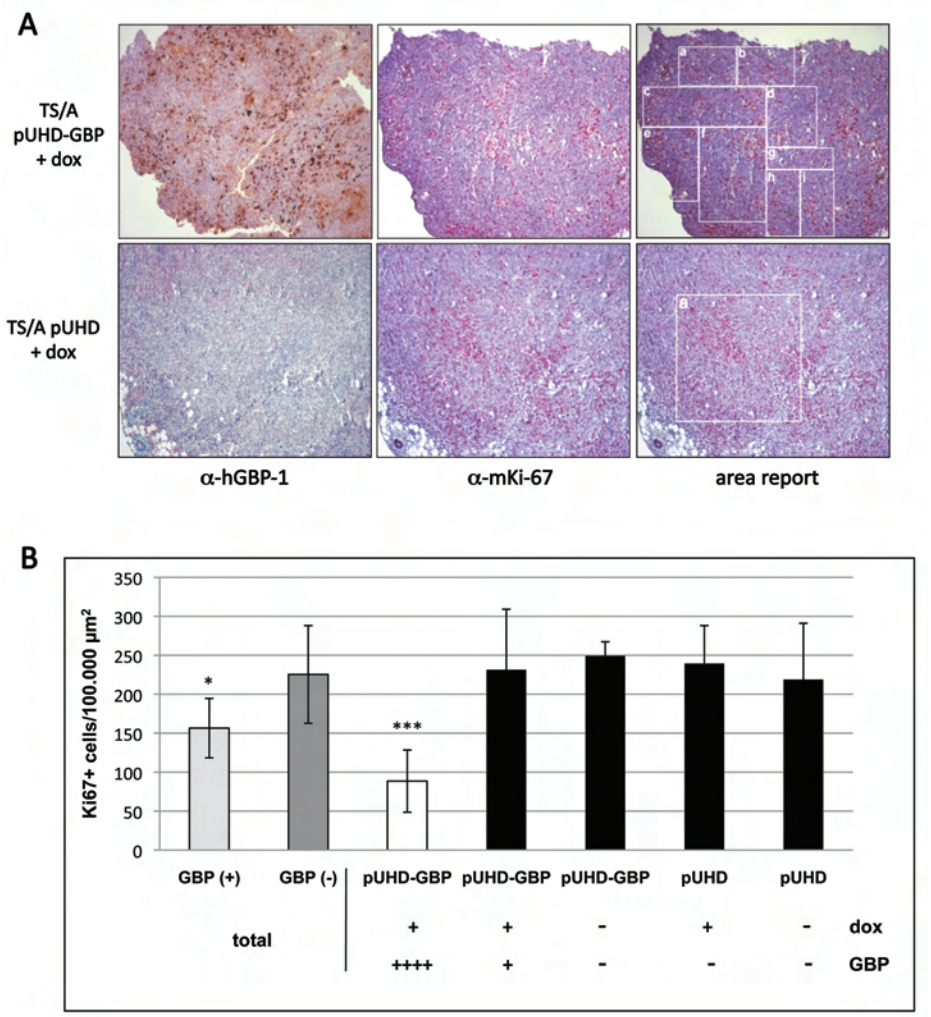

Figure 3. Evaluation of effects of hGBP-1 expression on tumor cell proliferation. (A) Immunohistochemistry. Consecutive sections of hGBP-1–expressing (TS/A-GBP + dox) and nonexpressing (TS/A-Hyg + dox) tumors were stained for expression of hGBP-1 (α-hGBP-1, brown cytoplasmic staining) and murine Ki-67 (α-mKi-67, red nuclear staining), a cellular proliferation marker. Using the Zeiss AxioVision analysis software, sections were divided into different areas correlating with a high level (a, b, d, e, g, h, i) or low level (c, f) hGBP-1 expression. (B) The number of Ki-67–positive TS/A cells was calculated and expressed as mean values per 100.000 μm^2. Statistical analysis revealed significant differences ($P = 0.017$) in the number of Ki-67–positive cells (mean values ± SD) in hGBP-1–expressing (total GBP^+, $n = 11$) compared with nonexpressing tumors (total GBP^-, $n = 10$). Highly significant differences ($P < 0.0001$, one-way ANOVA) were observed when Ki-67–positive cell numbers were correlated with hGBP-1 expression levels.

inserts). Altogether, no significant differences in lymphocyte cell numbers were observed in hGBP-1–expressing tumors in comparison to the respective saline-treated controls (see Figure 4). Moreover, evaluation of hematoxylin/eosin–stained sections did not reveal any signs of inflammation. Thus, these results indicate that the observed growth reduction in hGBP-1–expressing tumors in this syngeneic mouse model is not due to an elevated immune response.

Reduced Tumor Growth Corresponds with Decreased Hemoglobin Contents and Reduced VEGF-A Levels *in vitro* and *in vivo*

Finally, to investigate vascularization in TS/A cell–derived tumors, corresponding tumor sections were stained for expression of hGBP-1 and murine CD31, a molecular marker of endothelial cells (33). By this means, all tumors were shown to be well vascularized with few necrotic areas (Figure 5A). Quantitative analyses, which were performed to evaluate microvessel densities in hGBP-expressing tumors compared with nonexpressing tumors, did not reveal any statistically significant differences (data not shown). To determine the qualitative capacity of the newly formed tumor vessels to supply the respective tissue with oxygen and nutrients, the amount of hemoglobin was determined in tumors with and without hGBP-1 expression (Figure 5B). This well-established method is applied to quantify the actual state of perfusion within a given tumor tissue (34,35). For each group of tumors, 18 samples were analyzed. Interestingly, a significantly lower amount of hemoglobin was determined in tumor samples expressing hGBP-1 in comparison to nonexpressing tumors ($P = 0.0032$), indicating that hGBP-1 expression in tumor cells may impair their capabilities to promote tissue vascularization. Thus, to address potential indirect effects of hGBP-1 on angiogenesis, VEGF release from hGBP-1–expressing and nonexpressing tumor cells was determined by application of an ELISA specific for the detection of murine VEGF-A. Two independent cell clones (14 and 18) were investigated and showed a 20–60% decrease of secreted VEGF-A when hGBP-1 expression was induced by doxycycline (Figure 6A). In comparison, mock-transfected cells (TS/A pUHD) under the applied conditions showed a 5–25% reduced release of VEGF-A. To investigate the VEGF-A protein levels in corresponding mammary tumors, 12 different samples, derived from animals transplanted with pUHD-GBP–transfected

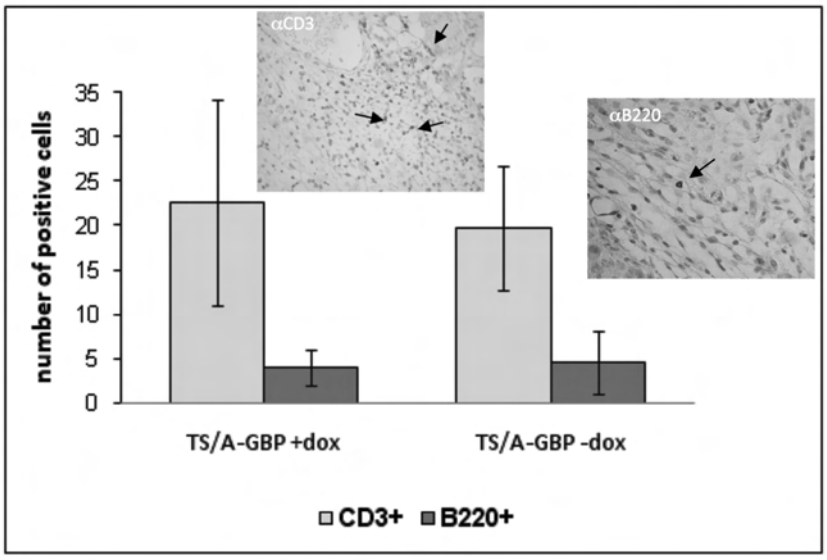

Figure 4. Quantification of tumor infiltration. Sections of TS/A-pUHD10.3-GBP–derived tumors from four different animals that had been treated with doxycycline (TS/A-GBP + dox) or saline (TS/A-GBP – dox) were analyzed by immunohistochemistry for the presence of $CD3^+$ T cells or $B220^+$ B cells. In both experiments, 10 different optical fields were evaluated. Results are indicated as mean values ± SD. No statistically significant differences were observed. Examples of successful staining are shown (inserts).

TS/A cells that were treated with either doxycycline or saline, were subjected to quantitative Western blot analysis (Figure 6B). After normalization to loaded protein amounts as reflected by GAPDH-specific staining, VEGF-A protein levels in hGBP-expressing tumors in average were shown to be significantly lower ($P = 0.0286$) than in the respective mock-treated controls (see Figure 6B). This result indicates that hGBP-1 may inhibit VEGF-A release from tumor cells, which may in turn result in decreased tumor vascularization and inhibition of tumor cell proliferation *in vivo*.

DISCUSSION

IFN-γ coordinates diverse cellular programs through transcriptional regulation of immunologically relevant genes. Multiple cellular effects of IFN-γ have been described, including upregulation of pathogen recognition, antigen processing and presentation, immune modulation and leukocyte trafficking, and induction of the antiviral state as well as inhibition of cellular proliferation and effects on apoptosis (36). The latter effects have been implicated in the more recently acknowledged antitumoral activities of IFN-γ, in addition to an IFN-γ–mediated tumor angiostasis and initiation of antitumoral innate and adoptive immune responses (1). Within the broad spectrum of IFN-γ–induced genes, those encoding GBPs are among the most abundant. In humans, hGBP-1 is the major IFN-γ–induced protein (32,37). Initial observations indicated an antiviral activity (38) of this molecule; however, within the last few years a major role of hGBP-1 in the regulation of endothelial cell function has been demonstrated. Thus, hGBP-1 was shown to inhibit proliferation (17) and migration (19) as well as capillary formation and invasiveness (16) of endothelial cells and is required to transfer the antiangiogenic activities of inflammatory cytokines such as IFN-γ, IL-1 and tumor necrosis factor (TNF)-α onto endothelial cells (16,17,19). In addition, recent evidence is accumulating showing that hGBP-1 is involved in antitumoral response processes. In a study involving 388 patients with colorectal carcinomas (20), robust hGBP-1 expression was detected in 30% of the tumors in endothelial cells and monocytes of the desmoplastic stroma. Most interestingly, this finding was associated with a reduced tumor angiogenesis and a highly significantly improved prognosis for the patients (20). Although GBPs from other species, mice in particular, are less well studied with respect to their biological function, an antitumorigenic activity of murine GBP-1 has been recently suggested by a significant upregulation of the respective gene in prostate tumors, which regressed during IFN-α therapy (39). This finding corresponds to previous work implicating IFN-γ–induced murine GBP-1 in the regression of mammary carcinomas in a Balb/c-derived tumor mouse model (7). Moreover, an antiproliferative effect of IFN-γ has been described for normal human mammary epithelial cells, and interestingly, mammary cancer cell lines with missing or reduced GBP-1 expression have been demonstrated to be resistant to IFN-γ–induced growth arrest (40).

In the present study, using an inducible, IFN-γ–independent expression system, we could demonstrate that hGBP-1 significantly inhibits the growth of highly malignant TS/A mammary carcinoma cells in syngeneic immune-competent Balb/c mice *in vivo*. In light of previous data described above, this finding might suggest concordant functions of murine and human GBP-1. The hGBP-1–mediated antitumorigenic effect in this model was associated with reduced tumor cell proliferation, as demonstrated by a significantly decreased number of Ki-67–positive cells in TS/A cell–derived tumors expressing high levels of hGBP-1 (see Figure 3B). Because hGBP-1 expression *in vitro* affected neither tumor cell proliferation nor tumorigenicity (see Figure 1B, C), the effects observed *in vivo* are most likely due to more indirect, paracrine effects. In this respect, effects resulting from interactions of tumor cells with the surrounding stroma or potential immune reactions are of particular inter-

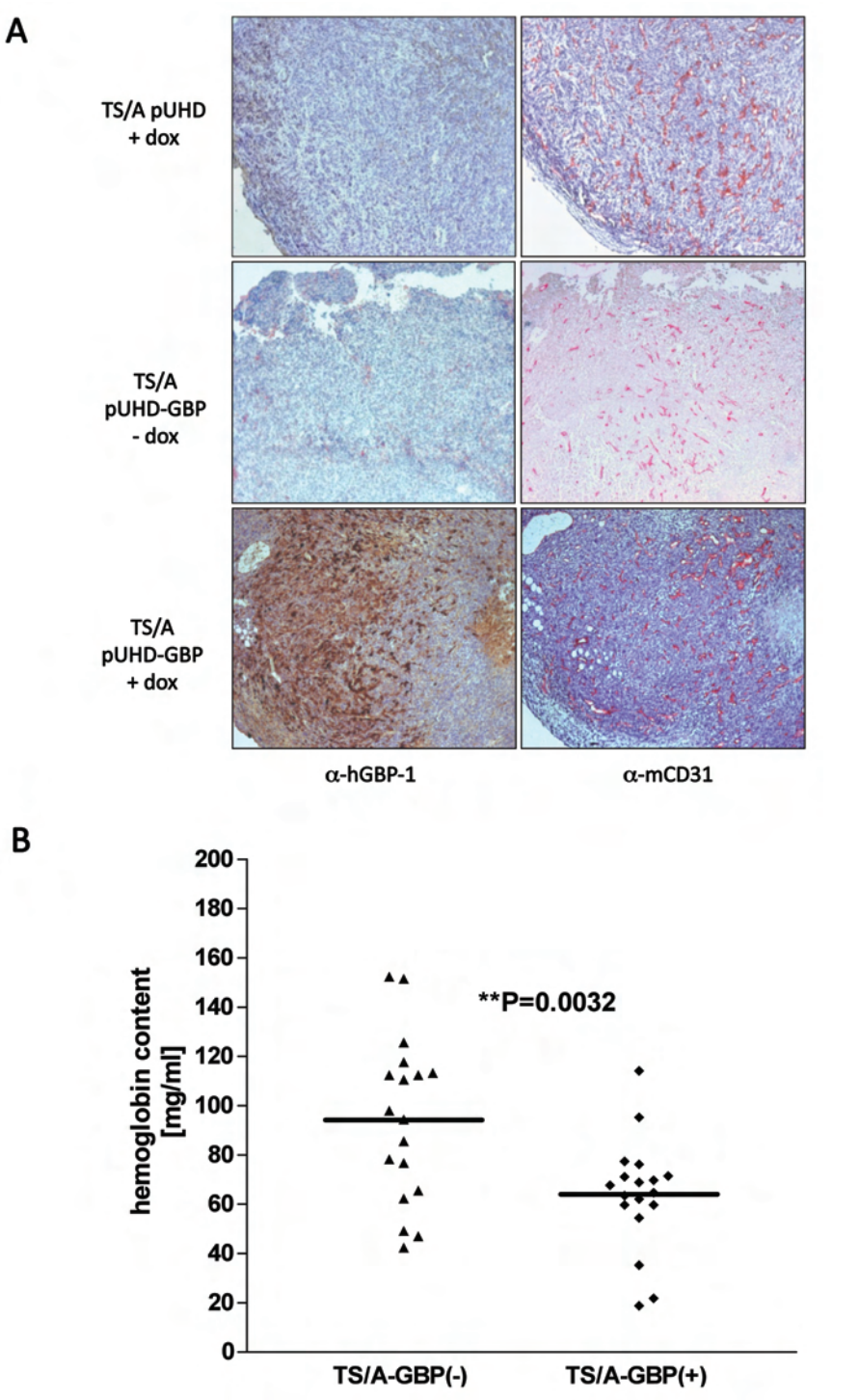

Figure 5. Analysis of tumor angiogenesis. (A) Immunohistochemistry. Consecutive sections of hGBP-1–expressing (TS/A-GBP + dox) and nonexpressing (TS/A-Hyg + dox, TS/A-GBP – dox) tumors were stained for the presence of hGBP-1 (α-hGBP-1, brown cytoplasmic staining) and CD31 (α-mCD31), a specific marker of endothelial cells (red staining). (B) Biochemical determination of hemoglobin contents. The amount of hemoglobin, normalized to total protein amounts, was determined in frozen tissue (n = 18) of hGBP-1–expressing (TS/A-GBP$^+$) and nonexpressing (TS/A-GBP$^-$) tumors. Statistical significance (P = 0.0032) of the encountered differences was shown by applying an unpaired Student t test.

est. The immune response in the present study was investigated at the T- and B-cell level. Evaluation of immunohistochemical analyses revealed neither signs of inflammation nor elevated levels of infiltrating lymphocytes (see Figure 4). Interestingly, analysis of tumor angiogenesis revealed significantly reduced concentrations of hemoglobin in tumors expressing hGBP-1 compared with nonexpressing samples (see Figure 5B). Because microvessel density was not affected (data not shown), however, this result indicates that quality rather than quantity of tumor vasculature might be impaired. Unlike normal blood vessels, tumor vessels are often immature and of irregular shape and diameter, and reveal an increased permeability. This may result in an increased interstitial fluid pressure and decreased perfusion (41,42). One of the major molecules regulating blood vessel formation and function is VEGF-A. It controls proliferation, survival and migration of endothelial cells as well as angiogenic sprouting (43). By analyzing the release of VEGF-A from hGBP-1–expressing TS/A cells *in vitro* (see Figure 6A), a marked decrease (up to 60%) was observed in comparison to nonexpressing cells. The slight decrease (5–25%) observed in mock-treated TS/A cells lacking the hGBP-1 expression construct might reflect reduced cellular metabolic activities under the applied conditions. Quantitative analysis of VEGF-A protein levels in tumor samples by means of Western blotting (see Figure 6B) consistently revealed a significantly reduced amount of VEGF-A in hGBP-1–expressing tumors compared with mock-treated controls. Significantly lower hemoglobin levels, indicating less tissue perfusion in accordance with a significantly reduced tumor cell proliferation, as observed in hGBP-1 expressing tumors, suggests that an hGBP-1–mediated decrease in VEGF-A synthesis may account for reduced angiogenesis and tumor growth *in vivo*. The underlying detailed mechanisms and how IFN-mediated effects might add to this antitumorigenic activity will be the subject of further investigations.

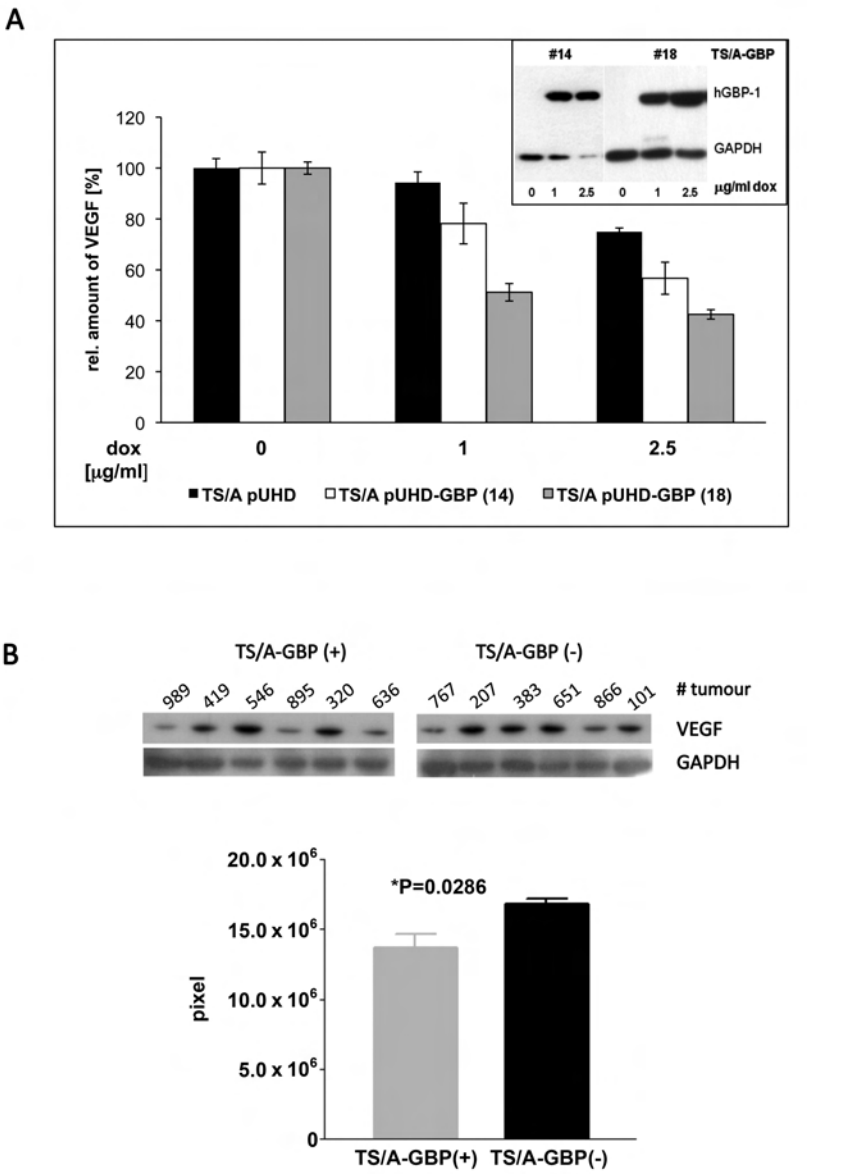

Figure 6. Effect of hGBP-1 expression on VEGF-A synthesis. (A) The Tet-regulated hGBP-1–expressing TS/A cell clones 14 and 18, which were used for generation of subcutaneous tumors in Balb/c mice, were analyzed for VEGF-A synthesis applying a mouse-specific ELISA. As a control, cells harboring the parental vector pUHD were used. Cells (duplicates) were cultured for 96 h in the presence of doxycycline (1 and 2.5 μg/mL), and the respective cell culture supernatants were analyzed. Obtained values (mean ± SD) were normalized to cell numbers (1×10^6) and set in relation to values obtained with nontreated cells (0 μg/mL dox). Corresponding cell extracts were analyzed for hGBP-1 expression by Western blotting (insert). (B) Quantitative Western blot analysis of VEGF-A in TS/A cell–derived tumor samples. Frozen tissue samples ($n = 6$) of tumors grown in mice that had received doxycycline for induction of hGBP-1 expression (TS/A-GBP$^+$) or were injected with saline (TS/A-GBP$^-$) were subjected to Western blot analysis to detect murine VEGF-A protein. GAPDH was stained as an internal control to monitor the amount of loaded protein. Quantification of band intensities was performed with the ImageQuant software. Background corrected single values were normalized to measurements of GAPDH-specific bands and summarized, and the mean values (± SEM) were compared for statistically significant differences by applying an unpaired Student *t* test. The calculated *P* value is indicated.

In summary, we have demonstrated that hGBP-1 may significantly contribute to an antitumoral response reaction of the host. Although the ectopic high-level expression in the present study might not reflect a physiological situation, recent reports have demonstrated hGBP-1 expression in human prostate cancers in stroma (including endothelial and inflammatory cells), as well as in tumor cells (39). Similar findings were obtained analyzing samples of human cholangiocellular carcinomas (our unpublished data). The mechanisms underlying this antitumorigenic effect may include autocrine processes affecting cell proliferation, but also paracrine activities affecting the expression and release of protumorigenic factors such as VEGF. Thus, owing to these activities, GBPs may represent potent members of an innate, IFN-γ–induced antitumoral defense system.

ACKNOWLEDGMENTS

We acknowledge the excellent technical assistance of Doris Rosenfellner and Melanie Nurtsch in immunohistochemistry. We also thank Daniel Portsmouth for critical reading of the manuscript. This work was partially funded by the ZIT program co-operate Vienna 2003 (to C Hohenadl and M Stürzl) and by grants of the Interdisciplinary Center of Clinical Research (IZKF) of the University of Erlangen, the Deutsche Forschungsgemeinschaft (DFG 317/2-1) and the Federal Ministry of Education and Research (BMBF, Polyprobe Study) to M Stürzl.

DISCLOSURE

The authors declare that they have no competing interests as defined by *Molecular Medicine*, or other interests that might be perceived to influence the results and discussion reported in this paper.

REFERENCES

1. Dunn GP, Koebel CM, Schreiber RD. (2006) Interferons, immunity and cancer immunoediting. *Nat. Rev. Immunol.* 6:836–48.
2. Kim R, Emi M, Tanabe K. (2007) Cancer immunoediting from immune surveillance to immune escape. *Immunology* 121:1–14.

3. Dighe AS, Richards E, Old LJ, Schreiber RD. (1994) Enhanced in vivo growth and resistance to rejection of tumor cells expressing dominant negative IFN gamma receptors. *Immunity* 1:447–56.
4. Kaplan DH, *et al.* (1998) Demonstration of an interferon gamma-dependent tumor surveillance system in immunocompetent mice. *Proc. Natl. Acad. Sci. U. S. A.* 95:7556–61.
5. Kundu N, Beaty TL, Jackson MJ, Fulton AM. (1996) Antimetastatic and antitumor activities of interleukin 10 in a murine model of breast cancer. *J. Natl. Cancer Inst.* 88:536–41.
6. Kundu N, *et al.* (1998) Interleukin-10 gene transfer inhibits murine mammary tumors and elevates nitric oxide. *Int. J. Cancer* 76:713–9.
7. Sun H, Jackson MJ, Kundu N, Fulton AM. (1999) Interleukin-10 gene transfer activates interferon-gamma and the interferon-gamma-inducible genes Gbp-1/Mag-1 and Mig-1 in mammary tumors. *Int. J. Cancer* 80:624–9.
8. Walser TC, *et al.* (2007) Immune-mediated modulation of breast cancer growth and metastasis by the chemokine Mig (CXCL9) in a murine model. *J. Immunother.* 30:490–8.
9. Cheng YS, Colonno RJ, Yin FH. (1983) Interferon induction of fibroblast proteins with guanylate binding activity. *J. Biol. Chem.* 258:7746–50.
10. Vestal DJ. (2005) The guanylate-binding proteins (GBPs): proinflammatory cytokine-induced members of the dynamin superfamily with unique GTPase activity. *J. Interferon Cytokine Res.* 25:435–43.
11. Kresse A, *et al.* (2008) Analyses of murine GBP homology clusters based on in silico, in vitro and in vivo studies. *BMC Genomics* 9:158.
12. Degrandi D, *et al.* (2007) Extensive characterization of IFN-induced GTPases mGBP1 to mGBP10 involved in host defense. *J. Immunol.* 179:7729–40.
13. Olszewski MA, Gray J, Vestal DJ. (2006) In silico genomic analysis of the human and murine guanylate-binding protein (GBP) gene clusters. *J. Interferon Cytokine Res.* 26:328–52.
14. Prakash B, Renault L, Praefcke GJ, Herrmann C, Wittinghofer A. (2000) Triphosphate structure of guanylate-binding protein 1 and implications for nucleotide binding and GTPase mechanism. *EMBO J.* 19:4555–64.
15. Prakash B, Praefcke GJ, Renault L, Wittinghofer A, Herrmann C. (2000) Structure of human guanylate-binding protein 1 representing a unique class of GTP-binding proteins. *Nature* 403:567–71.
16. Guenzi E, *et al.* (2003) The guanylate binding protein-1 GTPase controls the invasive and angiogenic capability of endothelial cells through inhibition of MMP-1 expression. *EMBO J.* 22:3772–82.
17. Guenzi E, *et al.* (2001) The helical domain of GBP-1 mediates the inhibition of endothelial cell proliferation by inflammatory cytokines. *EMBO J.* 20:5568–77.
18. Naschberger E, Bauer M, Stürzl M. (2005) Human guanylate binding protein-1 (hGBP-1) characterizes and establishes a non-angiogenic endothelial cell activation phenotype in inflammatory diseases. *Adv. Enzyme Regul.* 45:215–27.
19. Weinländer K, *et al.* (2008) Guanylate binding protein-1 inhibits spreading and migration of endothelial cells through induction of integrin alpha4 expression. *FASEB J.* 22:4168–78.
20. Naschberger E, *et al.* (2008) Angiostatic immune reaction in colorectal carcinoma: impact on survival and perspectives for antiangiogenic therapy. *Int. J. Cancer* 123:2120–9.
21. Gorbacheva VY, Lindner D, Sen GC, Vestal DJ. (2002) The interferon (IFN)-induced GTPase, mGBP-2: role in IFN-gamma-induced murine fibroblast proliferation. *J. Biol. Chem.* 277:6080–7.
22. Nanni P, de Giovanni C, Lollini PL, Nicoletti G, Prodi G. (1983) TS/A: a new metastasizing cell line from a BALB/c spontaneous mammary adenocarcinoma. *Clin. Exp. Metastasis* 1:373–80.
23. Ausserlechner MJ, Obexer P, Deutschmann A, Geiger K, Kofler R. (2006) A retroviral expression system based on tetracycline-regulated tricistronic transactivator/repressor vectors for functional analyses of antiproliferative and toxic genes. *Mol. Cancer Ther.* 5:1927–34.
24. Agu CA, *et al.* (2006) The cytotoxic activity of the bacteriophage lambda-holin protein reduces tumour growth rates in mammary cancer cell xenograft models. *J. Gene Med.* 8:229–41.
25. Naschberger E, *et al.* (2006) Human guanylate binding protein-1 is a secreted GTPase present in increased concentrations in the cerebrospinal fluid of patients with bacterial meningitis. *Am. J. Pathol.* 169:1088–99.
26. Lubeseder-Martellato C, *et al.* (2002) Guanylate-binding protein-1 expression is selectively induced by inflammatory cytokines and is an activation marker of endothelial cells during inflammatory diseases. *Am. J. Pathol.* 161:1749–59.
27. Zabala M, *et al.* (2004) Optimization of the Tet-on system to regulate interleukin 12 expression in the liver for the treatment of hepatic tumors. *Cancer Res.* 64:2799–804.
28. Beckstead JH. (1994) A simple technique for preservation of fixation-sensitive antigens in paraffin-embedded tissues. *J. Histochem. Cytochem.* 42:1127–34.
29. Beckstead JH. (1995) A simple technique for preservation of fixation-sensitive antigens in paraffin-embedded tissues: addendum. *J. Histochem. Cytochem.* 43:345.
30. Zeng G, Gao L, Birkle S, Yu RK. (2000) Suppression of ganglioside GD3 expression in a rat F-11 tumor cell line reduces tumor growth, angiogenesis, and vascular endothelial growth factor production. *Cancer Res.* 60:6670–76.
31. Urruticoechea A, Smith IE, Dowsett M. (2005) Proliferation marker Ki-67 in early breast cancer. *J. Clin. Oncol.* 23:7212–20.
32. Naschberger E, *et al.* (2004) Nuclear factor-kappaB motif and interferon-alpha-stimulated response element co-operate in the activation of guanylate-binding protein-1 expression by inflammatory cytokines in endothelial cells. *Biochem. J.* 379:409–20.
33. Baluk P, McDonald DM. (2008) Markers for microscopic imaging of lymphangiogenesis and angiogenesis. *Ann. N. Y. Acad. Sci.* 1131:1–12.
34. Russo A, *et al.* (2005) Inhibition of granuloma-associated angiogenesis by controlling mast cell mediator release: role of mast cell protease-5. *Br. J. Pharmacol.* 145:24–33.
35. Norrby K. (2006) In vivo models of angiogenesis. *J. Cell Mol. Med.* 10:588–612.
36. Schroder K, Hertzog PJ, Ravasi T, Hume DA. (2004) Interferon-gamma: an overview of signals, mechanisms and functions. *J. Leukoc. Biol.* 75:163–89.
37. Tripal P, Bauer M, Naschberger E, *et al.* (2007) Unique features of different members of the human guanylate-binding protein family. *J. Interferon Cytokine Res.* 27:44–52.
38. Anderson S, Carton J, Lou J, Xing L, Rubin B. (1999) Interferon-induced guanylate binding protein-1 (GBP-1) mediates an antiviral effect against vesicular stomatitis virus and encephalomyocarditis virus. *Virology* 256:8–14.
39. Persano L, *et al.* (2009) Interferon-alpha counteracts the angiogenic switch and reduces tumor cell proliferation in a spontaneous model of prostatic cancer. *Carcinogenesis* 30:851–60.
40. Harvat BL, Jetten AM. (1996) Gamma-interferon induces an irreversible growth arrest in mid-G1 in mammary epithelial cells which correlates with a block in hyperphosphorylation of retinoblastoma. *Cell Growth Differ.* 7:289–300.
41. Jain RK. (2005) Normalization of tumor vasculature: an emerging concept in antiangiogenic therapy. *Science* 307:58–62.
42. Jain RK. (2003) Molecular regulation of vessel maturation. *Nat. Med.* 9:685–93.
43. Ellis LM, Hicklin DJ. (2008) VEGF-targeted therapy: mechanisms of anti-tumour activity. *Nat. Rev. Cancer* 8:579–91.